British Journal of Pharmacology (2009), 157, 281–293

0007-1188/09
www.brjpharmacol.org

RESEARCH PAPER

Pharmacological characterization of PF-00547659, an anti-human MAdCAM monoclonal antibody

N Pullen[1], E Molloy[2], D Carter[1], P Syntin[3], F Clemo[4], D Finco-Kent[4], W Reagan[4], S Zhao[4], T Kawabata[4] and S Sreckovic[1]

[1]*Pfizer Global Research and Development, Sandwich, Kent, UK,* [2]*J&J PRD, High Wycombe Bucks, UK,* [3]*Novartis Vaccines and Diagnostics Via Fiorentina, Siena, Italy, and* [4]*Pfizer Global Research and Development, Groton, CT, USA*

Background and purpose: The adhesion molecule mucosal addressin cell adhesion molecule (MAdCAM) plays an essential role in the recruitment of lymphocytes to specialized high endothelial venules of the gastrointestinal tract and in their excessive tissue extravasation observed in inflammatory conditions, such as Crohn's disease. We have characterized the *in vitro* pharmacological properties of two monoclonal antibodies blocking MAdCAM, MECA-367 and PF-00547659, and determined their pharmacokinetic/pharmacodynamic profiles *in vivo*.
Experimental approach: Functional adhesion assays and surface plasmon resonance were used to characterize, *in vitro*, the pharmacological properties of MECA-367 and PF-00547659. The *in vivo* effects of MECA-367 and PF-00547659 on restriction of β_7^+ memory T lymphocytes were determined in mice and macaques, respectively, over the pharmacological dose range to confirm pharmacokinetic/pharmacodynamic relationships.
Key results: MECA-367 and PF-00547659 bound with high affinity to mouse and human MAdCAM with K_d values of 5.1 and 16.1 pmol·L^{-1} respectively and blocked the adhesion of $\alpha_4\beta_7^+$ leukocytes to MAdCAM with similar potency. MECA-367 and PF-00547659 induced a similar, dose-dependent two- to threefold increase in circulating populations of β_7^+ memory T-cells in the mouse and macaque; without affecting the β_7^- populations.
Conclusions and implications: PF-00547659 has potential utility in the treatment of inflammatory conditions by blocking tissue homing of activated $\alpha_4\beta_7^+$ leukocytes. The characterization of a rodent cross-reacting antibody as a surrogate for PF-00547659 in the search for potential pharmacological biomarkers and the determination of efficacious doses was effective in addressing the restricted orthologous cross-reactivity of PF-00547659 and the challenges this poses with respect to efficacy and safety testing.
British Journal of Pharmacology (2009) **157**, 281–293; doi:10.1111/j.1476-5381.2009.00137.x; published online 2 April 2009

Keywords: inflammatory bowel disease; MAdCAM; PK/PD; leukocyte homing; PF-00547659; MECA-367

Abbreviations: ELISA, enzyme-linked immunosorbent assay; FACS, fluorescence-activated cell sorting; GALT, gut-associated lymphoid tissue; IBD, inflammatory bowel disease; LPAM, lymphocyte Peyer's patch adhesion molecule (integrin $\alpha_4\beta_7$); MAdCAM, mucosal addressin cell adhesion molecule; PD, pharmacodynamic; PK, pharmacokinetic; PML, progressive multifocal leukoencephalopathy; VCAM, vascular cell adhesion molecule

Introduction

The selectivity of lymphocyte homing to specialized lymphoid tissue (Peyer's patches and mesenteric lymph nodes) and mucosal sites of the gastrointestinal tract is determined by the expression on endothelial cells of the mucosal addressin cell adhesion molecule, MAdCAM (Streeter *et al.*, 1988; Nakache *et al.*, 1989; Briskin *et al.*, 1997). MAdCAM is a member of the immunoglobulin superfamily (Shyjan *et al.*, 1996) and supports the specific rolling, adhesion and diapedesis of leukocytes bearing the integrin $\alpha_4\beta_7$ (also known as LPAM) (Berlin *et al.*, 1993; Erle *et al.*, 1994) to the specialized endothelium of the gastrointestinal tract. Tumour necrosis factor α (TNFα) and other pro-inflammatory cytokines increase endothelial MAdCAM expression and, in biopsy specimens taken from patients with Crohn's disease and ulcerative colitis, there is an approximate two- to threefold focal increase in MAdCAM expression at sites of inflammation (Briskin *et al.*, 1997; Souza *et al.*, 1999; Arihiro *et al.*, 2002). Its expression appears to be tightly linked with a physiological role in normal immune surveillance in the gut, but under conditions of chronic gastrointestinal tract inflammation, it appears to facilitate excessive lymphocyte extravasation, thus contributing to mucosal damage.

Correspondence: Dr Nick Pullen, Pfizer PGRD, Ramsgate Road, Sandwich, Kent CT13 9NJ, UK. E-mail: nick.pullen@pfizer.com
Received 26 September 2008; revised 6 November 2008; accepted 12 November 2008

The generation of a rat anti-mouse MAdCAM monoclonal antibody, MECA-367 (Streeter *et al.*, 1988), has contributed considerably to the understanding of the role of MAdCAM in pathological states in preclinical inflammatory disease models (Picarella *et al.*, 1997; Hanninen *et al.*, 1998; Barrett *et al.*, 2000; Kanwar *et al.*, 2000; Kato *et al.*, 2000; Shigematsu *et al.*, 2001). In several preclinical colitis models, for instance, blockade of MAdCAM/$\alpha_4\beta_7$ reduced lymphocyte recruitment, mucosal destruction and clinical signs (Hesterberg *et al.*, 1996; Picarella *et al.*, 1997; Kato *et al.*, 2000; Hokari *et al.*, 2001; Shigematsu *et al.*, 2001; Farkas *et al.*, 2006; Goto *et al.*, 2006; Apostolaki *et al.*, 2008), suggesting that targeting this axis might have utility in the treatment of inflammatory bowel disease (IBD).

Antibodies are proving to be an important class of drugs for treatment of chronic diseases and especially IBD. For example, the anti-TNFα blocking antibodies infliximab, adalimumab and, more recently, certolizumab reduce exacerbations and corticosteroid use in patients with Crohn's disease (Behm and Bickston, 2008) and dramatically improve patient's lives. Despite this progress, a substantial proportion of patients lack an initial or durable response to anti-TNFα treatment and there is an enduring concern over the long term safety and elevated risk of opportunistic infections of this class of immune suppressants (Lin *et al.*, 2008). Natalizumab is a humanized anti-α_4 integrin blocking monoclonal antibody approved for induction and maintenance treatment of moderate to severe Crohn's disease refractory to conventional therapies (Sandborn *et al.*, 2005; Targan *et al.*, 2007). Initially approved in 2004, for the treatment of multiple sclerosis, natalizumab was temporarily withdrawn from the market after three patients developed progressive multifocal leukoencephalopathy (PML; Van Assche *et al.*, 2005) caused by reactivation of dormant JC virus. Natalizumab has a potentially wide repertoire of function, blocking both $\alpha_4\beta_1$ and $\alpha_4\beta_7$ leukocyte interactions. As $\alpha_4\beta_1$/vascular cell adhesion molecule (VCAM)-dependent processes appear to predominate in the recruitment of leukocytes for immune surveillance of the central nervous system (CNS) (Engelhardt *et al.*, 1998; Engelhardt, 2006), the possibility that the blockade of the $\alpha_4\beta_1$ processes directly contributes to the increased risk of PML in the patient population taking natalizumab cannot be ruled out.

Here, we describe the identification and characterization of PF-00547659, a fully human anti-human MAdCAM $IgG_{2\kappa}$ monoclonal antibody and contrast its *in vitro* and *in vivo* pharmacological profile with MECA-367, in order to build confidence in the pharmacokinetic/pharmacodynamic (PK/PD) relationship and dose estimates for efficacy in man.

Methods

Animals

All animal care complied fully with UK legislation and with EEC and Italian Guidelines for Laboratory Animal Welfare. Experimental protocols were approved by local ethical review.

Recombinant reagents

Two immunogens were prepared for immunization of the XenoMouse™ mice (Green, 1999), a soluble human MAdCAM-IgG_1 Fc fusion protein and membranes of NIH-3T3 cells stably transfected with human MAdCAM (hMAdCAM). The hMAdCAM-IgG_1 Fc fusion protein was prepared by cloning a EcoRI/BglII cDNA fragment, encoding the mature extracellular, immunoglobulin-like domain of hMAdCAM, from an Incyte clone (3279276) into EcoRI/BamHI sites of the pIG1 vector (Simmons, 1993). The hMAdCAM-IgG_1 Fc fusion protein cDNA was cloned into pCDNA3.1+ for stable expression in CHO-DHFR cells. For protein expression, a hollow fibre bioreactor was seeded with stably expressing hMAdCAM-IgG_1 Fc CHO cells in Iscove's media containing 10% low IgG fetal bovine serum (FBS), non-essential amino acids, 2 mmol·L^{-1} glutamine, sodium pyruvate, 100 μg·mL^{-1} G418 and 100 ng·mL^{-1} methotrexate, and used to generate concentrated media supernatant. The hMAdCAM-IgG_1 Fc fusion protein was purified from the harvested supernatant by affinity chromatography on HiTrap Protein G Sepharose, size-exclusion by Sephacryl S100 column, and finally anion-exchange chromatography (Resource Q) using standard techniques. For use as an immunogen and all subsequent assays, the material was buffer exchanged into 25 mmol·L^{-1} HEPES pH 7.5, 1 mmol·L^{-1} ethylene diamine tetraacetic acid (EDTA), 1 mmol·L^{-1} dithiothreitol, 100 mmol·L^{-1} NaCl, 50% glycerol and stored as aliquots at –80°C. A soluble mouse MAdCAM (mMAdCAM) IgG_1 Fc fusion protein was generated in a similar way by reverse transcription polymerase chain reaction (RT-PCR) using primers against the known cDNA sequence (Streeter *et al.*, 1988), cloning into a pIG1 vector, generation of stable CHO cell transformants and affinity purification from hollow fibre bioreactor supernatant as described above.

In NIH-3T3 and CHO cells stably expressing hMAdCAM, a full length hMAdCAM-1a cDNA was generated by cloning a SacI/NotI PCR fragment, comprising nucleotides 645–1222 of the published MAdCAM sequence (Shyjan *et al.*, 1996), from a colon cDNA library into SacI/NotI sites of pIND-Hygro vector (Invitrogen) and splicing a SacI fragment, comprising the additional 5′ coding sequence from pCDNA3.1 hMAdCAM-IgG_1 Fc. A KpnI/NotI fragment containing the MAdCAM cDNA was then cloned into corresponding sites in a pEF5FRTV5GWCAT vector (Invitrogen), replacing the CAT coding sequence and used in transfections to generate single stably expressing clones in FlpIn NIH 3T3 cells and FlpIn CHO cells (Invitrogen) according to the manufacturer's instructions. Stably expressing clones were selected by their ability to support the binding of a $\alpha_4\beta_7^+$ JY human B lymphoblastoid cell line (Chan *et al.*, 1992), outlined below and expanded in roller bottles. hMAdCAM-expressing FlpIn NIH-3T3 cells were grown in Dulbecco's modified Eagle's medium containing 2 mmol·L^{-1} L-glutamine, 10% donor calf serum and 200 μg·mL^{-1} hygromycin B and expanded in roller bottles. MAdCAM-expressing FlpIn CHO cells were grown in Ham's F12/Dulbecco's modified Eagle's medium, containing 2 mmol·L^{-1} L-glutamine, 10% donor calf serum and 350 μg·mL^{-1} hygromycin B. Cells were harvested by use of a non-enzymatic cell dissociation solution and scraping, washing in phosphate buffered saline by centrifugation. Cell membranes were prepared from the cell pellet by two rounds of Polytron homogenization in 25 mmol·L^{-1} BisTris pH 8, 10 mmol·L^{-1} $MgCl_2$, 0.015% (w/v) aprotinin, 100 U·mL^{-1} bacitracin and centrifugation. The final pellet was resuspended in

the same buffer, and 50×10^6 cell equivalents aliquoted into thick-walled Eppendorf centrifuge tubes and centrifuged at >100 000× *g* to generate cell membrane pellets for XenoMouse™ mice immunizations. Supernatant was decanted and membranes were stored in these tubes at –80°C until required.

A CHO line expressing a chimeric fusion protein of the extracellular domain of the cynomolgus macaque MAdCAM (cMAdCAM) and the hMAdCAM stalk domain was generated as follows: the cMAdCAM extracellular domain was generated by RT-PCR from mesenteric lymph node mRNA using 5′ AGCATGGATCGGGGCCTGGCC and 3′ GTGCAGGACCGGGATGGCCTG primers and cloned into pCR2.1-TOPO (Invitrogen); a SacI fragment was then spliced in frame into the pIND-Hygro vector containing the hMAdCAM C-terminal domain as described above; A KpnI/NotI fragment containing the cyno-humanMAdCAM cDNA was then cloned into corresponding sites in a pEF5FRTV5GWCAT vector and used in transfections to generate single stably expressing clones in FlpIn CHO cells according to the manufacturer's instructions. Stably expressing clones were selected by their ability to support the binding of a $\alpha_4\beta_7^+$ JY human B lymphoblastoid cell line (Chan *et al*., 1992).

Immunization and hybridoma generation

Eight to 10 week old XenoMouse™ mice (Green, 1999) were immunized intraperitoneally or in their hind footpads with either the purified recombinant hMAdCAM-IgG_1 Fc fusion protein (10 μg per dose per mouse), or cell membranes prepared from NIH 3T3 cells (10×10^6 cells per dose per mouse). This dose was repeated five to seven times over a 3 to 8 week period. Four days before fusion, the mice received a final injection of MAdCAM-IgG_1 Fc fusion protein in phosphate buffered saline (PBS). Spleen and lymph node lymphocytes from immunized mice were fused with the non-secretory myeloma P3-X63-Ag8.653 cell line and were subjected to HAT selection as previously described (Galfre and Milstein, 1981). A panel of hybridomas all secreting MAdCAM specific human $IgG_{2\kappa}$ and $IgG_{4\kappa}$ antibodies were recovered and sub-cloned; a hybridoma clone secreting PF-00547659 was selected for further evaluation on the basis of its enzyme-linked immunosorbent assay (ELISA) and pharmacological profile using assays described below.

Assays

Detection of antigen-specific antibodies in mouse serum and hybridoma supernatant was determined by ELISA using hMAdCAM-IgG_1 Fc fusion protein to capture the antibodies and for non-specific reactivity against human IgG_1. Briefly, ELISA plates were coated overnight at 4°C with 100 μL per well of hMAdCAM-IgG_1 Fc fusion (4.5 μg·mL^{-1}) in 100 mmol·L^{-1} sodium carbonate/bicarbonate buffer pH 9.6. Plates were blocked with 5% bovine serum albumin (BSA), 0.1% Tween-20, in PBS and incubated at room temperature for 1 h. Blocking buffer was removed and 50 μL per well of hybridoma supernatant or purified PF-00547659 was added for 2 h at room temperature. The plate was then washed with PBS (3 × 100 μL per well) and monoclonal antibody (mAb) binding detected with horseradish peroxidase (HRP)-conjugated secondary antibodies (1:1000 in PBS). The plates were incubated at room temperature for 1 h, washed in PBS (3 × 100 μL per well) and finally developed with o-phenylenediamine (DAKO) solution (0.67 mg·mL^{-1}) containing 0.0125% (v/v) H_2O_2 (100 μL per well). The plates were allowed to develop, the reaction stopped with 2 mol·L^{-1} H_2SO_4 and the plates read at 490 nmol·L^{-1}. The specificity of PF-00547659 binding to hMAdCAM over other cell adhesion molecules was compared by ELISA with soluble mMAdCAM, VCAM and fibronectin protein.

Antibodies that demonstrated binding to hMAdCAM-IgG_1 Fc fusion protein by ELISA were assessed for antagonist activity in an adhesion assays with $\alpha_4\beta_7^+$ JY cells and either hMAdCAM-IgG_1 Fc fusion protein or MAdCAM-CHO cells. For the hMAdCAM-IgG_1 Fc fusion assay, purified hMAdCAM-IgG_1 Fc fusion protein (100 μL of 4.5 μg·mL^{-1} stock) in Dulbecco's PBS was adsorbed to 96-well Black Microfluor 'B' U-bottom plates overnight at 4°C. Plates were blocked for at least 1 h at 37°C in 10% BSA/PBS. JY cells were cultured in RPMI 1640 containing 2 mmol·L^{-1} L-glutamine and 10% heat-inactivated FBS and seeded at 1–2 × 10^5 cells·mL^{-1} every 2–3 days to prevent the culture from differentiating. During this time, cultured JY cells were loaded with Calcein AM (5 μmol·L^{-1} final concentration; 37°C for 30 min) in RPMI 1640 and antibody dilutions prepared to determine IC_{50} potency. After blocking, 50 μL of antibodies/controls were added to each well and the plate incubated at 37°C for 20 min. Calcein-loaded JY cells were washed with RPMI 1640 + 10% FBS and 1 mg·mL^{-1} BSA/PBS by centrifugation, resuspending the final cell pellet to 1×10^6 cells·mL^{-1} in 1 mg·mL^{-1} BSA/PBS. 100 μL of cells were added to each well of the U bottomed plate, the plate sealed, briefly centrifuged (450× *g* for 2 min) and the plate then incubated at 37°C for 45 min. The plates were washed to remove unbound JY cells (Skatron plate washer) and fluorescence measured (excitation λ485 nm, emission λ535 nm). A similar assay was employed to determine the IC_{50} potency of MECA-367 (Nakache *et al*., 1989) for mMAdCAM-IgG_1 Fc fusion protein. The IC_{50} value was defined as the antibody concentration at which the adhesion response had decreased to 50% of the response in the absence of anti-MAdCAM antibody.

For the cell–cell adhesion assays, recombinant stable transformants of hMAdCAM and cyno-human MAdCAM CHO cells were used. Cells were seeded at 4×10^4 cells per well in 96-well black plates – clear bottom and cultured overnight at 37°C/5% CO_2. Purified PF-00547659 dilutions were made in 1 mg·mL^{-1} BSA/PBS and aliquots (50 μL) incubated at 37°C for 20 min, prior to incubation (45 min) with Calcein AM-loaded JY cells (100 μL of 1×10^6 mL^{-1} in 1 mg·mL^{-1} BSA/PBS as described above), then added to the plate after the 20 min incubation period with the antibody. The plate was then washed (Tecan plate washer) and fluorescence measured as above to determine the IC_{50} potency.

BIAcore derived affinity constant determination

An affinity measure was determined by surface plasmon resonance using the BIAcore 3000 instrument, following the manufacturer's protocols. Affinity purified PF-00547659 or MECA-367 were immobilized onto the dextran layer of a CM5

biosensor chip using amine coupling. Samples of hMAdCAM-IgG_1 or mMAdCAM-IgG_1 Fc fusion protein in running buffer were prepared at concentrations ranging from 1–30 nmol·L^{-1}. Samples were randomized and injected in triplicate for 3 min each across four flow cells with 10 mmol·L^{-1} HEPES pH 7.4, 150 mmol·L^{-1} NaCl, 3 mmol·L^{-1} EDTA, 0.005% Surfactant P20. A flow rate of 100 µL·min^{-1} was used to minimize mass transport limitations. Dissociation of MAdCAM-IgG_1 Fc fusion protein was monitored for 180 min and the surface regenerated by either a 24 s injection of 40 mmol·L^{-1} H_3PO_4 or a 6 s injection of 25 mmol·L^{-1} H_3PO_4 (50 µL·min^{-1}). On and off-rate data were analysed using the BIAevaluation (V3.1) software package on the BIAcore 3000.

PF-00547659 generation

Hybridoma cells, expressing PF-00547659, were seeded at 2 × 10^5 cells·mL^{-1} and grown in a spinner culture containing BD quantum yield, 15% low IgG heat-inactivated FBS, 1% 100× non-essential amino acid solution, 10 U·mL^{-1} interleukin–6 (IL–6) and OPI media supplement at 37°C/5% CO_2. When maximum viable cell density was reached, Optimab was added, as per manufacturer's instructions, to enhance antibody secretion. Cell viability was monitored, and the media harvested by centrifugation when the viability dropped to below 20%. Hybridoma supernatant was harvested and PF-00547659 was purified by HiTrap Protein G affinity chromatography. PF-00547659 was buffer exchanged into 20 mmol·L^{-1} NaOAc, 140 mmol·L^{-1} NaCl, pH 5.5, using a 26/10 desalting column. Once buffer exchanged, PF-00547659 was filtered through 0.22 µm filter in a cell culture hood, to ensure sterility, and stored at 4°C.

Immunophenotyping

For mice dosed with MECA-367, changes in circulating levels of $CD4^+LPAM^+$ memory T-cells were determined by fluorescence-activated cell sorting (FACS). Blood was lysed with Pharmlyse according to manufacturer's instructions, by incubation in the dark at room temperature (15 min). Cells were centrifuged (450× *g*; 15 min) and the pellet resuspended in PBS/1% BSA to the equivalent starting blood volume. Aliquots (ca. 450 µL) were labelled with anti-mouse $\alpha_4\beta_7$/LPAM, CD4 and CD45Rb; the remaining sample was pooled for monocolour controls. Cells were labelled in the dark (1 h), centrifuged (450× *g*, 15 min at 4°C) to pellet cells. Samples were resuspended (0.5 mL), in PBS/1% BSA for FACS analysis (FACSScan); percentages of $LPAM^-$ and $LPAM^+$ $CD4^+CD45Rb^{low}$ memory T-cells were determined for all MECA-367 doses compared with isotype control animals. Haematological parameters in cynomolgus blood were determined using an Advia haematology system according to the manufacturer's instructions. Absolute numbers and % population of T, B and natural killer (NK) cells as well as granulocytes and monocytes in peripheral blood (100 µL) were measured using a FACSCalibur flow cytometer according to the manufacturer's instructions by differential staining of CD3, CD4, CD8, CD16 and CD20 and compared with Streck biological control. Absolute numbers and % population of $CD4^+\beta_7^+CD95^{lo}CD28^+$ (naïve), $CD4^+\beta_7^+CD95^{hi}CD28^+$ (central memory), $CD4^+\beta_7^-CD95^{hi}CD28^+$ (central memory) and $CD4^+\beta_7^+CD95^{hi}CD28^-$ (effector memory) lymphocyte subsets were measured (Pitcher *et al.*, 2002). Blood (100 µL) or Streck control was incubated with the appropriate antibody (30 µL) for 20–30 min at 4°C. FACSlyse solution (1 mL of 1:10) was added to each tube and the tube briefly vortexed at low/moderate speed. The tubes were incubated at room for approximately 12 min in the dark, not exceeding 20 min. To ensure the complete lysis, the opacity of each tube was checked, and then an additional 500 µL of FACSlyse was added to tubes that appeared cloudy. Streck control samples were more resistant to lysis and often required an additional 500 µL of lyse solution. BD stain buffer (2 mL) was added to each tube, briefly vortexed and centrifuged at 250× *g* for 6–7 min at room temperature. The supernatant was decanted and the cell pellet re-suspended in staining buffer (3 mL) and centrifuged at 250× *g* for 6–7 min at room temperature. Cytofix buffer (100 µL), a neutral pH-buffered saline that contains 4% w/v paraformaldehyde, was added to the cell pellets from monkey peripheral blood and mixed thoroughly. Cytofix buffer was not added to the Streck control samples. The samples were kept at 4°C in the dark until acquisition by FACSCalibur. For acquisition, the instrument settings were optimized to bring lymphocyte population on scale, compensating each channel (FITC, PE, PerCP and APC) individually. For each tube, 20 000 lymphocyte (R1) events were collected.

The % and absolute cell counts for the haematology, immunophenotyping and lymphocyte subsets for each of the time points, as well as the two pre-dose controls were determined for each animal and for all doses of PF-00547659. The fold increases in circulating populations of leukocytes as well as the $CD4^+\beta_7^+CD95^{lo}CD28^+$ (naïve), $CD4^+\beta_7^+CD95^{hi}CD28^+$ (central memory), $CD4^+\beta_7^-CD95^{hi}CD28^+$ (central memory) and $CD4^+\beta_7^+CD95^{hi}CD28^-$ (effector memory) T-cell subsets for each of the time points over the pre-dose controls were determined for each animal dosed with PF-00547659. Statistically significant changes were measured using the ANOVA Labstats add-in to Excel.

Effect of MECA-367 on $LPAM^+$ leukocytes in the mouse

FVB mice were purchased from Charles River UK. Single increasing doses of MECA-367 or IgG_2 isotype control (0.1, 0.3, 1, 3 mg·kg^{-1}) were administered by intravenous tail vein to $n = 8$ cohorts of FVB mice in saline (20 µL per mouse). At day 7 post dosing, animals were killed by lethal overdose of anesthetic, and total blood samples were collected in a heparinized syringe from the posterior vena cava for FACS analysis as described above.

Effect of PF-00547659 on β_7^+ leukocyte subsets in the cynomolgus macaque

Male and female captive-bred cynomolgus monkeys (Macaca fascicularis; Nerviano Medical Science S.r.l) were used for this study. The presence of any pre-existing anti-PF-00547659 antibodies was determined by primate anti-human antibody (PAHA) assay and only animals with negative reactions in the PAHA assay were used in this study. Animals were randomly assigned to treatment groups ($n = 2$ per sex per group) Blood

(2.5 mL in 8% EDTA) was also collected at 1, 3, 6, 10 and 14 days after dosing and used within 8 h of collection for haematology, immunophenotyping and to determine the distribution of populations of $CD4^+\beta_7^+CD95^{lo}CD28^+$ (naïve), $CD4^+\beta_7^+CD95^{hi}CD28^+$ (central memory), $CD4^+\beta_7^-CD95^{hi}CD28^+$ (central memory) and $CD4^+\beta_7^+CD95^{hi}CD28^-$ (effector memory) T-cells by flow cytometry. Samples were maintained at room temperature and processed to determine levels of lymphocytes within 6 h of sample collection. The distribution of $CD4^+\beta_7$ populations of T-cells was determined by flow cytometry and compared with the pre-dose levels. Two pre-dose blood samples were used to evaluate the levels of circulating lymphocytes and those subsets relevant to the PD endpoints.

PF-00547659 (0.01, 0.05, 0.1 and 1 mg·kg^{-1}) was administered in solution (11.3 mg·mL^{-1} PF-00547659 in 20 mmol·L^{-1} sodium acetate, 45 mg·mL^{-1} mannitol, 0.02 mg·mL^{-1} disodium EDTA dihydrate, 0.2 mg·mL^{-1} polysorbate-80; pH 5.5) as an intravenous bolus.

PF-00547659 PK levels

The levels of PF-00547659 were determined at 1, 2, 6 and 24 h, then 3 (72 h), 6, 10 and 14 days after dosing. Blood samples (2.5 mL) were collected in serum separator tubes and PF-00547659 levels in serum were determined by enzyme ELISA by modification of the assay described above. hMAdCAM-IgG_1 Fc capture antigen (100 µL) to a final concentration of 1 µg·mL^{-1} in coating buffer (0.05 mol·L^{-1} carbonate-bicarbonate buffer, pH 9.6) was coated on to 96-well plates and incubated overnight at 4°C. In order to obtain a standard curve, PF-00547659 was diluted in PBS containing 5% (w/v) bovine serum albumin and 0.5% (v/v) Tween-20 (PBSTB) to 0.5, 5, 20, 35, 50, 65, 80, 95, 110, 500, 1500 ng·mL^{-1}. ELISA plates were washed [6 × ~400 µL per well per wash with phosphate buffered saline containing 0.5% (v/v) Tween-20 (PBST)] and then blocked with PBSTB (150 µL per well) and incubated at room temperature for 1 h. Plates were washed (6 × ~400 µL with PBST) and then standards (100 µL), blank and test samples (sera diluted 1:20 in PBSTB) were dispensed to assay plates. The plates were sealed and incubated at room temperature for 1 h with gentle shaking, then washed (6 × ~400 µL with PBST). Biotinylated mouse anti-human IgG_2 diluted 1:4000 in PBSTB (100 µL) was added, the plate sealed and incubated at room temperature for 1 h with gentle shaking. The plates were washed (6 × ~400 µL with PBST), and then an HRP-conjugated streptavidin (1:100 000 in PBSTB) was added to each well (100 µL). The plates were sealed and incubated at room temperature for 25 min with gentle shaking. The plates were finally washed with PBST (6 × ~400 µL) and then developed with equilibrated 3.3′,5,5′-tetramethylbenzidine (100 µL) by incubation for about 10 min at room temperature. The reaction was stopped by the addition of 2 N H_2SO_4 (100 µL) and read at 450 nm (reference at 650 nm). The lower limit of quantification of the assay for PF-00547659 was 0.5 ng·mL^{-1}.

Data analysis

Pharmacokinetic calculations were carried out using a non-compartmental approach with the aid of WinNonlin package (version 3.1, Pharsight Inc., CA, USA) and Excel. PF-00547659 terminal half-life ($t_{½}$) was calculated by the formula $t_{½} = \ln(2)/\lambda z$, where $-\lambda z$ is the slope of the terminal linear phase of natural-log concentrations versus time curve. PF-00547659 area under the serum concentration versus time curve, AUC, was determined by the linear trapezoidal rule up to the last detectable concentration $C_{t(last)}$ at time $t_{(last)}$, and denoted $AUC_{0-t(last)}$ and extrapolated to infinity ($AUC_{0-\infty}$) assuming mono-exponential decay using the formula:

$$AUC_{0-\infty} = AUC_{0-t(last)} + \frac{C_{t(last)} * t_{1/2}}{\ln(2)}$$

Systemic clearance (C_L) and volume of distribution at steady state (V_{ss}) were calculated as follows:

$$C_L = \frac{Dose}{AUC_{0-\infty}}$$

$$V_{ss} = C_L * MRT \text{ (mean residence time)}$$

MAdCAM immunohistochemistry

PF-00547659 was biotinylated using EZ-Link Sulfo-NHS-Biotin (Pierce) and purified by gel filtration using manufacturer's instructions. A biotinylated anti-KLH IgG_2 antibody was prepared as a negative control. The presence of MAdCAM expression was determined by a direct immunoperoxidase procedure (Vector Laboratories) on acetone-fixed cryosections of human and cynomolgus tissues (n = 2–3 donors/tissue) supplied by Charles River Laboratories, Inc., Frederick, MD. Sections were rinsed PBS and endogenous peroxidase quenched by incubation of the slides with glucose oxidase (2 U·mL^{-1})-glucose (10 mmol·L^{-1}) and sodium azide (1 mmol·L^{-1}) for 1 h at 35°C. The slides were then rinsed twice with PBS, blocked with avidin solution (15 min), rinsed with PBS, followed by blocking with biotin solution (15 min) at room temperature, and rinsed with PBS. This was followed by incubation with a protein block, PBS + 0.5% casein; 1% BSA; and 1.5% normal human gamma globulins (20 min) designed to reduce non-specific binding. Biotinylated PF-00547659 (0.1 µg·mL^{-1} in PBS +1% BSA) was incubated for 1 h at room temperature, then washed twice with PBS + 0.05% Tween-20 and treated with the ABC Elite reagent (30 min). Slides were then rinsed twice with PBS + 0.05% Tween-20 and treated with 3,3′-diaminobenzidine tetrahydrochloride (4 min). All slides were counterstained with haematoxylin, dehydrated and coverslipped for interpretation. All slides were read by a pathologist to identify the tissue or cell type stained and intensity of staining [graded ± (equivocal), 1+ (weak), 2+ (moderate), 3+ (strong), 4+ (intense) or Neg (negative)].

Materials

All antibodies used in this study were purchased from BD Pharmingen: MECA-367; antibodies (isotpye controls: mouse IgG_3-FITC, IgG_1-PE, IgG_1-PerCP, IgG_1-APC, IgG_2-PE; leukocytes: mouse anti-CD3 IgG_3-FITC, anti-CD16 $IgG_1\kappa$-PE, anti-CD20 $IgG_{2b\kappa}$-PE, anti-CD4 PerCP and anti-CD8 IgG_1-APC; T-cell subsets: mouse $IgG_{1\kappa}$-FITC, $IgG_{2a\kappa}$-PE, IgG_1-PerCP, $IgG_{1\kappa}$-

APC, anti-CD28-FITC, anti-β_7-PE, CD95-APC, CD4-PerCP and CD8-PerCP) used for immunophenotyping cynomolgus peripheral blood; and antibodies used for mouse peripheral blood profiling: anti-mouse LPAM-PE, CD4 PerCP-Cy5.5 and CD45RB-FITC. Calcein AM was purchased from Molecular Probes.

Results

Isolation of PF-00547659 and comparison of pharmacological profile with MECA-367

PF-00547659 was isolated by screening hybridoma lines generated from Xenomice (Green, 1999) immunized with hMAdCAM-IgG_1 Fc fusion and membranes from stably transfected cells expressing human MAdCAM. The ability of PF-00547659 to inhibit the adhesion of $LPAM^+$ expressing cells to human MAdCAM was determined in two formats, a soluble hMAdCAM-IgG_1 Fc fusion protein cell adhesion assay and a similar assay with CHO cells stably expressing the full length MAdCAM-1 receptor (Shyjan *et al.*, 1996). PF-00547659 inhibited JY cell adhesion to hMAdCAM-IgG_1 Fc fusion protein and hMAdCAM expressing CHO cells with IC_{50} values as shown in Table 1. The differences in the IC_{50} values were attributed to the relative differences in active MAdCAM expression and extent of JY adhesion in the two assays. A chimeric cynomolgus macaque MAdCAM extracellular domain fused to the hMAdCAM-1 stalk domain was generated and stably expressed in CHO cells. PF-00547659 blocked the binding of JY cells to this chimera (Table 1) but did not bind to mMAdCAM-IgG_1 fusion protein or block JY cell adhesion to mMAdCAM-IgG_1 fusion protein (data not shown). No binding of PF-00547659 could be demonstrated for the closely homologous cell adhesion molecules fibronectin and VCAM. Surface plasmon resonance was used to determine that PF-00547659 binds MAdCAM with high affinity with a mean K_D of 16.1 pmol·L^{-1} (n = 5, 95% CI = 7, 37.2). The extent of binding to CHO cells expressing hMAdCAM or the chimeric cynomolgus/human MAdCAM was qualitatively identical as measured by flow cytometry (data not shown).

MECA-367 (Nakache *et al.*, 1989) has been used extensively to understand the contribution of MAdCAM in preclinical inflammatory disease models of, for example, colitis (Picarella *et al.*, 1997; Kato *et al.*, 2000), gastritis (Barrett *et al.*, 2000) and diabetes (Yang *et al.*, 1997; Hanninen *et al.*, 1998). The *in vitro* functional properties of MECA-367 were compared with PF-00547569 in both JY adhesion assays and by BIAcore affinity (Table 1). The functional potency and affinity of MECA-367 for mMAdCAM-IgG_1 Fc was highly comparable with PF-00547659 for hMAdCAM-IgG_1 Fc fusion protein, indicating that MECA-367 would be a good surrogate antibody to compare the efficacy, safety and toxicity associated with blocking MAdCAM/LPAM interactions with PF-00547659.

PF-00547659 tissue cross-reactivity

Tissue sections of human colon were used to confirm the specificity of PF-00547659 for binding MAdCAM expressed on the endothelium (Figure 1) by immunohistochemistry as reported elsewhere (Briskin *et al.*, 1997). A panel of tissues from different species was used to identify a relevant PF-00547659 cross-reacting species by immunohistochemistry for safety and efficacy testing. Of these, the cynomolgus macaque was selected as the relevant species (data not shown) and the comparative expression of MAdCAM between cynomolgus and human tissues was determined by immunohistochemistry using a biotinylated-PF-00547659. A biotinylated-anti-KLH IgG_2 antibody was used as a non-specific control. Examination of a panel of cynomolgus and human test tissue confirmed that PF-00547659 specifically decorated those endothelial cells which were found in gastrointestinal and associated lymphoid tissues (Table 2). With a few notable differences, the intensity and pattern of PF-00547659 staining in cynomolgus and human was very similar with specific MAdCAM expression demonstrated in endothelium of colon [lamina propria and gut-associated lymphoid tissue (GALT)], oesophagus (lamina propria), small intestine (lamina propria, GALT and submucosal blood vessels), stomach (lamina propria, GALT and submucosa), lymph node, pancreas, spleen and liver (portal areas). With few exceptions, there were some weak occasional endothelial staining of the bone marrow and moderate-strong occasional staining in tonsil of cynomolgus as well as occasional endothelial staining in liver, lung, urinary bladder and uterus in some human donor samples. No evidence of MAdCAM expression on the endothelium of CNS tissue (brain, eye,

Table 1 Pharmacological characterization of PF-00547659 in comparison with MECA-367

	PF-00547659	*MECA-367*
Antibody type	Human IgG_2 kappa class	Rat IgG_{2a} kappa class
Reactivity	Human and cynomolgus MAdCAM	Mouse MAdCAM
BIAcore binding to MAdCAM	hMAdCAM-IgG_1 Fc fusion K_D 16.1 pmol·L^{-1} (n = 5, CI = 7, 37.2)	mMAdCAM-IgG_1 Fc fusion K_D 5.1 pmol·L^{-1} (n = 2)
Inhibition of CHO-hMAdCAM binding to JY cells	IC_{50}, 0.457 μg·mL^{-1} (n = 34; 95% CI = 0.405, 0.516).	N.D.
Inhibition of CHO-cynoMAdCAM to JY cells	IC_{50}, 0.651 μg·mL^{-1} (n = 18, 95% CI = 0.566, 0.748)	N.D.
Inhibition of MAdCAM-IgG_1 Fc fusion protein to JY cells	hMAdCAM-IgG_1 Fc fusion IC_{50}, 0.037 μg·mL^{-1} (n = 32; 95% CI = 0.027, 0.052)	mMAdCAM-IgG_1 Fc fusion IC_{50}, 0.033 μg·mL^{-1} (n = 4; 95% CI = 0.021, 0.05)
Inhibition of fibronectin and VCAM binding to Jurkat T-cells	IC_{50}, >24.5 μg·mL^{-1}	N.D.

MAdCAM, mucosal addressin cell adhesion molecule; N.D., not determined; VCAM, vascular cell adhesion molecule.

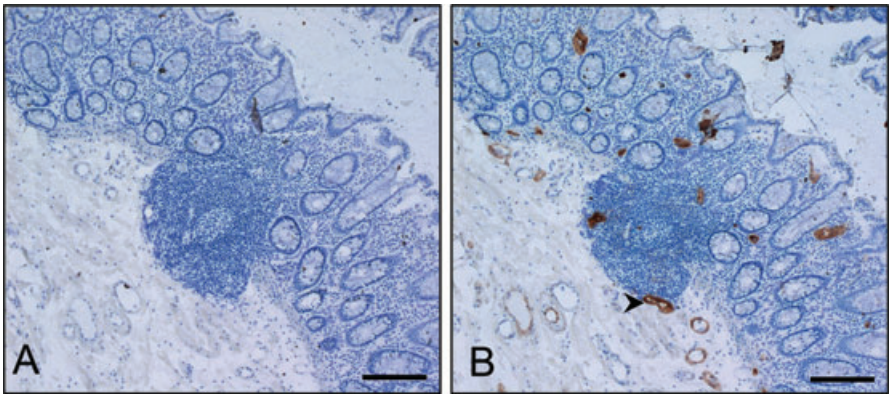

Figure 1 Immunohistochemical staining of endothelium expressing MAdCAM in human colon. (A) negative control, (B) PF-00547659 staining, arrows indicate specific endothelial staining in the gut lamina propria. The bar represents 200 μm. MAdCAM, mucosal addressin cell adhesion molecule.

Table 2 Pattern of cross-reactivity of PF-00547659 for cynomolgus and human tissues

	Cynomolgus	*Human*
Adrenal	Neg	Neg
Bone marrow	1+2/+	Neg
Brain (cerebellum, cortex, choroid plexus)	Neg	Neg
Breast	Neg	Neg
Colon (lamina propria and GALT endothelium)	2+ (2/2)	4+ (3/3)
Eye	Neg	Neg
Heart	Neg	Neg
Kidney	Neg	Neg
Liver (endothelium)	Neg	2+ (1/3)
Lung (endothelium)	Neg	3+ (1/3)
Lymph node (endothelium)	4+ (2/2)	4+ (3/3)
Oesophagus (endothelium)	3+ (1/2)	4+ (3/3)
Ovary	Neg	Neg
Pancreas (endothelium)	2+/3+	3+ (3/3)
Pituitary	Neg	Neg
Prostate	Neg	Neg
Skin	Neg	Neg
Small intestine (lamina propria and GALT endothelium)	3+ (2/2)	4+ (3/3)
Spinal cord	Neg	Neg
Spleen (endothelium)	3+ (2/2)	4+ (3/3)
Stomach (lamina propria and GALT endothelium)	3+ (2/2)	3+ (3/3)
Testis	Neg	Neg
Thymus	Neg	Neg
Tonsil (endothelium)	3+/4+	Neg
Ureter	Neg	Neg
Urinary bladder (endothelium)	Neg	2+ (1/3)
Uterus	Neg	1+ (1/3)

The extent of staining for each tissue was determined semi-quantitatively using the methodology as outlined in the methods. Where there was a difference in the staining intensity between samples from the same tissue, the individual scores are expressed. The number of tissues showing positive staining is shown in parentheses.
GALT, gut-associated lymphoid tissue.

pituitary), skin, sexual organs, heart or kidney was detected in cynomolgus or human samples.

Effect of MECA-367 on LPAM$^+$ cell populations in the mouse

The rat anti-mouse-MAdCAM mAb, MECA-367, blocks lymphocyte homing to the gut (Kato *et al.*, 2000; Farkas *et al.*, 2006; data not shown). The hypothesis that blockade of MAdCAM would result in an elevation of LPAM$^+$ ($\alpha_4\beta_7^+$) leukocytes in the peripheral circulation was tested by FACS. In a preliminary study, mice (n = 6) were given either MECA-367, or an isotype control IgG_2 antibody (1 mg·kg^{-1} *i.v.*). Three days post-dose, total blood was harvested, pooled and enriched white cell populations labelled with antibodies against CD4, CD45Rb and LPAM to confirm the pattern of cell distribution by FACS. Relatively low numbers of LPAM$^+$CD4$^+$CD45Rb^{low} memory T-cells were present in samples from animals given isotype control IgG_2 antibody (Figure 2A), but in samples of MECA-367 treated animals, the population of LPAM$^+$CD4$^+$CD45Rb^{low} memory T-cells were increased approximately twofold (Figure 2B). To confirm the dose response of this effect, mice (n = 8 per group) were given single increasing intravenous doses of MECA-367 or isotype control IgG_2 antibody (0.1, 0.3, 1 and 3 mg·kg^{-1}) and 7 days post-dose, blood samples were taken and levels of LPAM$^-$ and LPAM$^+$ CD4$^+$CD45Rb^{low} memory T-cell populations were determined by specific FACS assessment. Levels of LPAM$^-$ memory T-cells were unchanged regardless of treatment (data not shown), but there was a dose-dependent increase in circulating levels of LPAM$^+$ memory T-cells, with a maximal effect being observed at a dose of 1 mg·kg^{-1} (Figure 2C). The elevation in LPAM$^+$ memory T-cells was also accompanied by an increase in the relative LPAM staining (mean fluorescence intensity) on the cells, consistent with the notion that MAdCAM blockade was also able to displace high affinity LPAM$^+$ cells from MAdCAM interactions (compare Figure 2A with 2B). These observations were used to develop a biomarker assay that could be used to confirm the pharmacological effects of PF-00547659 in macaques and humans.

PK properties of PF-00547659 in the cynomolgus macaque

Increasing intravenous doses of PF-00547659 (0.01 mg·kg^{-1}–1 mg·kg^{-1}) were given to cynomolgus macaques and blood samples taken at time points up to 14 days post dosing to determine its PK profile. The pharmacokinetics were non-linear (Figure 3 and Table 3) with clearance decreasing as dose increased. A dose-dependent decrease in volume was observed

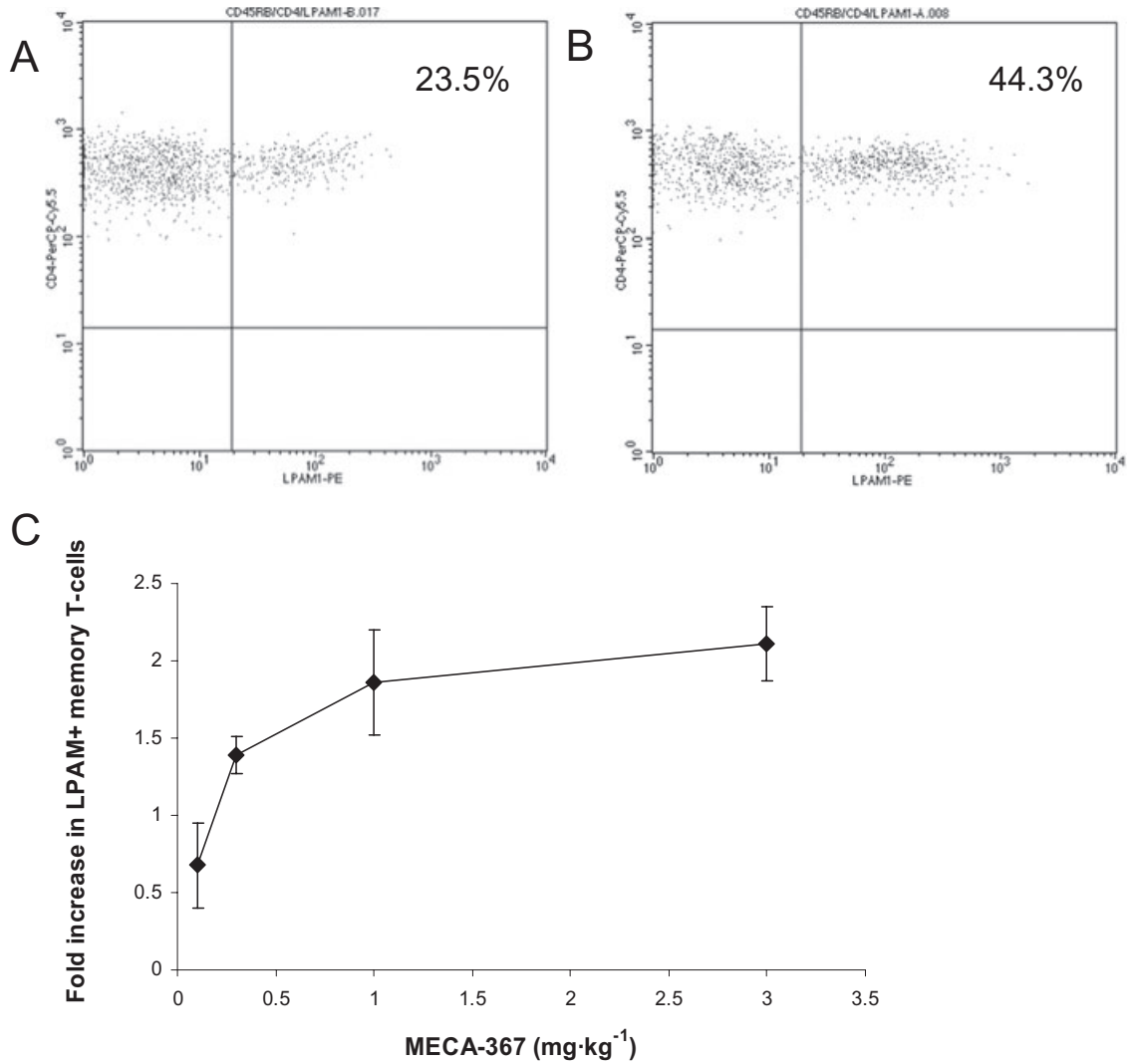

Figure 2 Dose-dependent changes in the population of LPAM$^+$CD4$^+$ memory T-cells in the peripheral circulation following intravenous doses of MECA-367 in the mouse. FVB mice were dosed (1 mg·kg^{-1} *i.v.*) with IgG_2 control mAb (A) or MECA-367 (B) and blood samples pooled 3 days post-dose analysed for LPAM$^+$CD4$^+$CD45Rb^{low} by flow cytometry. Data represent example dot plots, plotting the LPAM$^+$ populations of CD4$^+$CD45Rb cells. FVB mice were dosed with MECA-367 or IgG_2 control mAb (0.1, 0.3, 1 and 3 mg·kg^{-1}) and 7 days after dosing, levels of LPAM$^+$CD4$^+$ memory T-cells in each animal were determined by flow cytometry. Data (C) are plotted as fold changes compared with the isotype control as means ± SEM (n = 8). LPAM, lymphocyte Peyer's patch adhesion molecule (integrin $\alpha_4\beta_7$).

as dose increased, suggesting target-mediated change in disposition. The observed V_{ss} at the highest doses was similar to the plasma volume for monkeys (~40 mL·kg^{-1}) and suggests limited extravascular distribution. After a 0.01 mg·kg^{-1} dose, serum concentrations of PF-00547659 were only detectable up to 2 h post-dose and therefore PK parameters could not be accurately estimated. After 0.05 mg·kg^{-1}, the serum concentration-time profile declined bi-exponentially with serum levels detected up to 24 h post-dose. Systemic clearance was low, on average 2.7 mL·h^{-1}·kg^{-1} and the corresponding volume of distribution at steady state was 303 and 203 mL·kg^{-1} in males and females respectively. After 0.1 mg·kg^{-1}, serum concentrations declined in a bi-exponential manner with a half-life of 25 h. After 1 mg·kg^{-1}, the serum concentration-time profile was different from those after 0.05 and 0.1 mg·kg^{-1} doses, as mean PF-00547659 concentrations showed a plateau up to 144 h after dosing until serum concentrations dropped below 5000 ng·mL^{-1} and a more rapid terminal elimination phase was observed with a half-life of approximately 162 h. Mean systemic clearance values and volumes of distribution for all three doses are shown in Table 3.

PD changes in leukocyte populations

The changes observed in circulating levels of LPAM$^+$ T-cell populations to mice given MECA-367 (Figure 2) suggested a biomarker that could be used to follow the dose-effect relationship of PF-00547659 in preclinical species and humans, as measuring changes in recruitment of activated leukocytes to the gut is technically challenging and costly. Blood samples were collected both prior to and after (2, 4, 7, 11 and 15 days) PF-00547659 dosing. The absolute numbers of total lymphocytes, CD3$^+$, CD4$^+$ as well as CD8$^+$ T-cell lineages, CD20$^+$ B cells

and CD16$^+$ NK cells were determined using flow cytometry. At the highest intravenous dose of PF-00547659 (1 mg·kg^{-1}), there was a statistically significant increase of approximately 1.5-fold ($P < 0.005$) on the total number of lymphocytes in peripheral blood (Figure 4A). The duration of the response overlapped with the PK exposure depicted in Figure 3. Statistically significant increases in total lymphocytes were not clearly discernable for doses lower than 1 mg·kg^{-1}, but a similar magnitude and duration of response was observed for CD3$^+$ (Figure 4B, $P < 0.005$), CD4$^+$ (Figure 4C, $P < 0.005$) as well as CD8$^+$ (Figure 4D, $P < 0.005$) T-cell subsets and CD20$^+$ (Figure 4E, $P < 0.05$) B cell populations in animals dosed with PF-00547659 (1 mg·kg^{-1} *i.v.*). In contrast, there was no apparent effect on the numbers of CD16$^+$ NK cells in peripheral blood with PF-00547659 dosing (Figure 4F).

PD changes in populations of β_7^+ T-cells

A change in the population of circulating LPAM$^+$ T-cells was selected as a biomarker endpoint in the cynomolgus, as this would be a non-terminal endpoint and, building on similar data generated with the surrogate mAb in the mouse, it would generate data that could support the development of a PK/PD model and clinical dose-effect relationship for PF-00547659 for humans. A specific LPAM antibody was not available for these studies, so an antibody which recognizes the β_7 integrin was used to investigate the effect of PF-00547659 on circulating leukocyte populations further. The distribution of populations of CD4$^+\beta_7^+$CD95^{lo}CD28$^+$ (naïve), CD4$^+\beta_7^+$CD95^{hi}CD28$^+$ (central memory), CD4$^+\beta_7^-$CD95^{hi}CD28$^+$ (central memory) and CD4$^+\beta_7^+$CD95^{hi}CD28$^-$ (effector memory) T-cells was determined by flow cytometry. At baseline, approximately 34% of T-cells were CD4$^+$; of these 63% were naïve (of which ~87% β_7^+), 32% were central (of which ~41% β_7^+) and about 5% were effector T-cells (of which ~50% β_7^+) (data not shown) in cynomolgus macaques. Absolute numbers of these lymphocyte populations following single increasing doses of PF-00547659 were measured and the levels compared with the baseline control. The most durable and largest magnitude of effect on peripheral β_7^+ naïve, central and effector memory T-cell levels following PF-00547659 dosing was observed at the 1 mg·kg^{-1} dose level (Figure 5A–C) with a magnitude which was approximately two-, three- and 2.5-fold respectively. The variation in magnitude of response was greatest with the populations of β_7^+ naïve and effector T-cells, whereas the most robust and consistent responses were observed with the population of β_7^+ central memory T-cells. For this population of cells, increasing doses of PF-00547659 induced an approximate threefold increase of CD4$^+\beta_7^+$CD95^{hi}CD28$^+$ cells (Figure 5C) and a PD response which faithfully followed the PK profile depicted in Figure 3. In contrast, the population of β_7^- central memory T-cells remained unchanged from the pre-dose levels with increasing doses of PF-00547659 (Figure 5D), an effect which is consistent with the expected mechanism of action of PF-00547659.

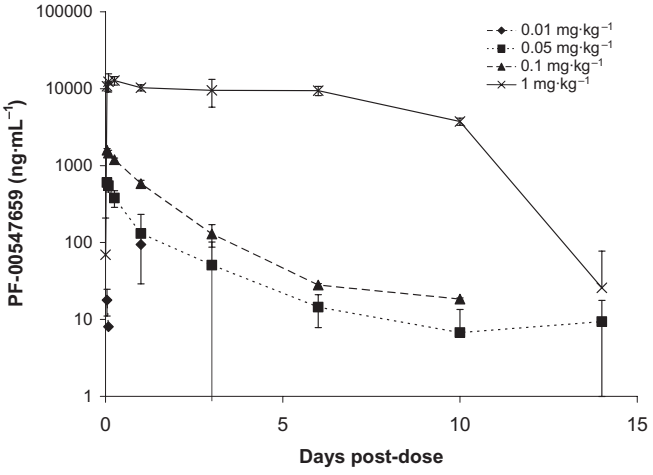

Figure 3 Mean serum concentration of PF-00547659 following increasing i.v. doses in cynomolgus macaques. Data are plotted as means ± SD ($n = 4$). Pharmacokinetic data from both males and females are represented together as a single mean.

Discussion

PF-00547659 is the first fully human blocking anti-MAdCAM mAb that has been identified and fully characterized. PF-00547659 was highly specific for cynomolgus and human MAdCAM over other homologous cell adhesion molecules

Table 3 Pharmacokinetic parameter estimates for PF-00547659 (using WinNonlin) in cynomolgus macaques following intravenous injection of a single dose (0.05–1 mg·kg^{-1})

Parameter	*Units*	*Dose (mg·kg^{-1})*					
		0.05		*0.1*		*1*	
		Mean	*SD*	*Mean*	*SD*	*Mean*	*SD*
Half-life_λz	H	29.07	13.48	24.93	0.71	162.20	11.29
T_{max}	H	1	0	1	0	2	2.2
C_{max}	ng·mL^{-1}	603	88	1591	77	14211	1970
C_0	ng·mL^{-1}	668	107	1747	122	12206	3170
Cl_{last}	mL·h^{-1} kg^{-1}	3.59	1.36	2.23	0.24	0.50	0.06
$AUC_{0\text{-}t(last)}$	μg·h·mL^{-1}	17.9	4.6	45.1	4.7	2041.9	264.8
MRT_{last}	H	26.46	8.66	38.50	1.62	105.81	3.36
V_{ss_last}	mL·kg^{-1}	131.52	43.40	85.70	6.87	52.47	6.86
V_{inital}	mL·kg^{-1}	76.20	11.44	57.46	3.95	86.24	22.22

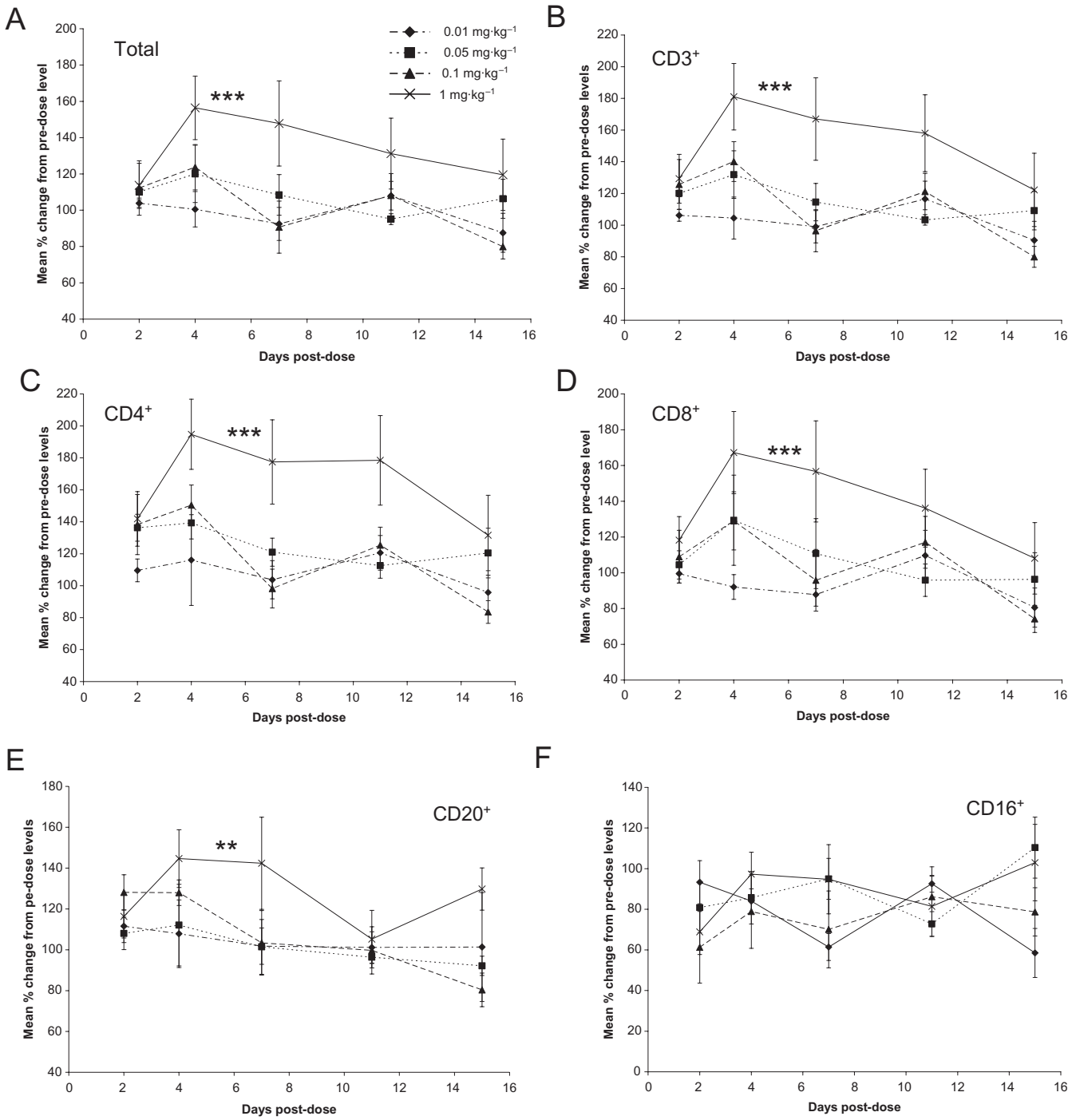

Figure 4 Changes in the levels of leukocyte populations over time in response to increasing doses of PF-00547659 over the pre-dose baseline in cynomolgus macaques. (A) mean % change in the absolute number of total lymphocytes. Data are plotted as means ± standard error of means (SEM; $n = 4$); ***$P < 0.005$ over 0.01 and 0.05 mg·kg^{-1} groups, $P = 0.01$ over 0.1 mg·kg^{-1} group; (B) mean % change in the absolute number of CD3$^+$ lymphocytes. Data are plotted as means ± SEM ($n = 4$); ***$P < 0.005$ over 0.01 and 0.01 mg·kg^{-1} groups, $P = 0.008$ over 0.05 mg·kg^{-1} group; (C) mean % change in the absolute number of CD4$^+$ lymphocytes. Data are plotted as means ± SEM ($n = 4$); ***$P < 0.005$ over 0.01 and 0.1 mg·kg^{-1} groups, $P = 0.009$ over 0.05 mg·kg^{-1} group; (D) mean % change in the absolute number of CD8$^+$ lymphocytes. Data are plotted as means ± SEM ($n = 4$); ***$P < 0.005$ over 0.01 mg·kg^{-1} group, $P < 0.05$ for 0.05 and 0.1 mg·kg^{-1} groups; (E) mean % change in the absolute number of CD20$^+$ lymphocytes. Data are plotted as means ± SEM ($n = 4$); **$P < 0.05$ over 0.01, 0.05 and 0.1 mg·kg^{-1} groups; (F) mean % change in the absolute number of CD16$^+$ lymphocytes. Data are plotted as means ± SEM ($n = 4$).

and in functional assays blocked the adhesion of LPAM bearing cells to cynomolgus and human MAdCAM with high potency (IC_{50} values of 0.651 and 0.457 μg·mL^{-1} respectively). A blocking rat anti-mouse MAdCAM mAb MECA-367 has been described (Streeter *et al.*, 1988; Nakache *et al.*, 1989) and used to understand the role of MAdCAM in inflammatory processes (Engelhardt *et al.*, 1998; Kato *et al.*, 2000; Shigematsu *et al.*, 2001; Arihiro *et al.*, 2002). While there are cur-

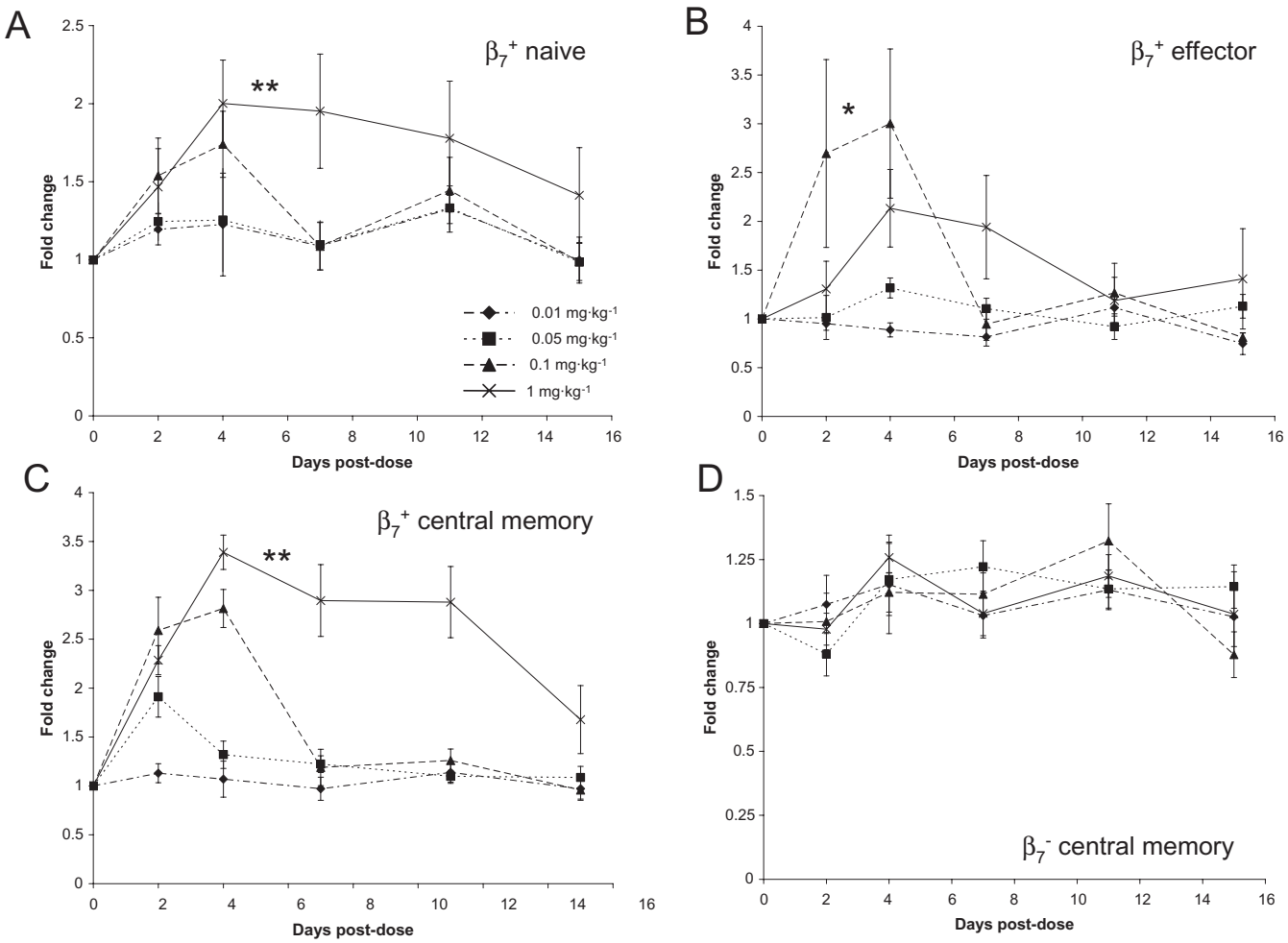

Figure 5 Fold change in β_7^+ populations of T-cells following increasing intravenous doses of PF-00547659 over pre-dose baseline levels in the cynomolgus macaque. (A) Mean fold change in the population of β_7^+ naive T-cells following escalating intravenous doses of PF-00547659 (0.01–1 mg·kg^{-1}) was determined by a change in the absolute cell number over the pre-dose levels. Data are plotted as means ± SEM (n = 4); **P = 0.007 and 0.009 for 0.01 and 0.05 mg·kg^{-1} groups respectively; (B) Mean fold change in the population of β_7^+ effector memory T-cells following escalating intravenous doses of PF-00547659 (0.01–1 mg·kg^{-1}). Data are plotted as means ± SEM (n = 4); *, p < 0.05 over the 0.01 mg/kg group; (C) Mean fold change in the population of β_7^+ central memory T-cells following escalating intravenous doses of PF-00547659 (0.01–1 mg·kg^{-1}), as determined by a change in the absolute cell number over the pre-dose levels. Data are plotted as means ± SEM (n = 4); **, p = 0.002 and 0.008 for 0.01 and 0.05 mg·kg^{-1} groups respectively; (D) Mean fold change in the population of β_7^- central memory T-cells following escalating intravenous doses of PF-00547659 (0.01–1 mg·kg^{-1}). Data are plotted as means ± SEM (n = 4).

rently no defined criteria to approve surrogate antibodies for use in safety testing, we undertook a rigorous *in vitro* and *in vivo* pharmacological evaluation of MECA-367 to determine its suitability as a surrogate antibody to support the clinical development of PF-00547659. Both the binding affinity and potencies of MECA-367 and PF-00547659 determined *in vitro* were highly comparable (Table 1), supporting the potential use of MECA-367 as a surrogate antibody for safety testing. Based on the ability of PF-00547659 and MECA-367 to block MAdCAM/$\alpha_4\beta_7$ interactions, it was hypothesized that escalating doses of anti-MAdCAM mAb might be expected to restrict gut homing $\alpha_4\beta_7^+$ leukocytes to the peripheral circulation. We compared the *in vivo* functional effects of MAdCAM blockade with MECA-367 to that with PF-00547659, by measuring the PD changes in LPAM$^+$ and β_7^+ populations of memory T-cells respectively. In the mouse, MECA-367 induced a dose-dependent increase in the number of circulating LPAM$^+$ memory T-cells with a maximal response between 1 and 3 mg·kg^{-1} compared with isotype control. In contrast, there was no change in the corresponding levels of LPAM$^-$ memory T-cells (data not shown), confirming the specificity of the effect. A similar study design and biomarker endpoint was used to confirm the dose-effect relationship of PF-00547659 in the cynomolgus macaque.

The non-compartmental pharmacokinetics of PF-00547659 indicated that the drug exhibits target mediated disposition, that is, binding to the receptor (MAdCAM) to the extent that the binding influences the disposition of the drug, as has been observed with other mAbs (Benincosa *et al.*, 2000; Mager and Jusko, 2001; Wu *et al.*, 2006; Mullamitha *et al.*, 2007). Target-mediated disposition was characterized by a dose-dependent decrease in the apparent volume of distribution as dose increased. In the case of target-mediated elimination, the non-linear characteristics of the concentration-time profiles

became more pronounced as concentration decreased, consistent with other observations from other mAbs (Benincosa *et al.*, 2000; Wu *et al.*, 2006; Mullamitha *et al.*, 2007). At concentrations above 5000 ng·mL^{-1} target-mediated disposition and elimination of PF-00547659 were negligible and the pharmacokinetics of PF-00547659 were similar to endogenous IgG_2 in monkeys. PF-00547659 did not substantially bind to mouse MAdCAM, but the PK effects observed in cynomolgus macaques were consistent with those observed with MECA-367 in mice (data not shown). A dose of 1 mg·kg^{-1}, PF-00547659 caused significant effects on total lymphocytes, as well as $CD3^+$, $CD4^+$, $CD8^+$ and $CD20^+$ cell populations in peripheral blood. In contrast, there was no apparent effect on the numbers of $CD16^+$ NK cells, potentially reflecting the low levels of expression of $\alpha_4\beta_7$ and adhesion to MAdCAM, observed for these cells (Erle *et al.*, 1994; Rott *et al.*, 2000). On β_7^+ cell populations, the effects of PF-00547659 were more marked with a sub-population of $CD4^+$ central memory T-cells showing the most robust and consistent increases in circulating levels after PF-00547659. In contrast, levels of β_7^- $CD4^+$ central memory T-cells remained unaltered with increasing doses of PF-00547659, in a manner consistent with the observations of MECA-367 in the mouse (data not shown). The PD effects of PF-00547659 on β_7^+ cell populations followed very closely the PK profile of PF-00547659 for each dose investigated, an effect that was also observed in mice dosed with MECA-367 (data not shown). The effect of PF-00547659 on β_7^+ central memory T-cells appeared to be sustained when serum levels of PF-00547659 were in excess of 100 ng·mL^{-1}. Taken together, the observations that MECA-367 and PF-00547659 have similar *in vitro* pharmacological profiles and comparable *in vivo* effects on blocking the recruitment of β_7^+ lymphocytes confirmed the utility of MECA-367 as a surrogate antibody for PF-00547659. That PF-00547659 has the expected pharmacological response in the cynomolgus macaque supports the use of this species as a relevant toxicology species and the biomarker data in modeling dose projections to humans.

Currently approved anti-TNFα therapies, such as infliximab, have considerable clinical value in the treatment of moderate to severe IBD, but their use increases the risk of severe opportunistic infections and malignancy (Lin *et al.*, 2008). Preclinical observations that blocking the gastrointestinal addressin MAdCAM and the recruitment of activated $\alpha_4\beta_7$-bearing lymphocytes to the gastrointestinal tract in IBD models improves disease outcome (Hesterberg *et al.*, 1996; Picarella *et al.*, 1997; Hokari *et al.*, 2001; Shigematsu *et al.*, 2001; Farkas *et al.*, 2006; Goto *et al.*, 2006; Apostolaki *et al.*, 2008), supports the notion that selective $\alpha_4\beta_7$/MAdCAM inhibition may be a desirable approach with potentially less immune suppression. As the founding member of a new class of agents for the induction and maintenance of remission in multiple sclerosis and Crohn's disease, the introduction of the anti-α_4 integrin mAb, natalizumab, has shown tremendous clinical promise, but its use has been also associated with rare lethal instances of re-activation of JC virus infection and PML (Van Assche *et al.*, 2005). Natalizumab blocks all α_4-mediated interactions including those with VCAM, fibronectin and MAdCAM (Andrew *et al.*, 1994). Preclinical studies have indicated that CNS immune surveillance is dominated by $\alpha_4\beta_1$/VCAM processes (Engelhardt *et al.*, 1998; Engelhardt, 2006). While there is some evidence of increased MAdCAM expression in the CNS in preclinical models of experimental autoimmune encephalomyelitis (Steffen *et al.*, 1996), evidence that MAdCAM plays a substantial role in the recruitment of immune cells under these conditions, compared with VCAM is missing. Immunohistochemical studies performed here with PF-00547659 have supported previous observations (Briskin *et al.*, 1997) that MAdCAM expression is spatially restricted in the adult to endothelial cells which line blood vessels in gastrointestinal and specialized lymphoid tissues; MAdCAM expression in the CNS (brain, spinal cord) was negligible. If one of the potential and desired effects of VCAM blockade by natalizumab for MS is to reduce recruitment of activated leukocytes to the CNS, then re-emergence of JC viral infection leading to PML may be one of the consequences of reduced immune surveillance. The mechanism of action of PF-00547659, by selectively binding MAdCAM and reducing homing of specific lineages of leukocytes to the gastrointestinal tract without impairing normal CNS immune surveillance, may be preferred as a therapeutic treatment for IBD.

As a template for others, the methodology and data presented here support the utility of well characterized surrogate antibodies in the development of novel biotherapeutics with restricted orthologous cross-reactivity.

Acknowledgements

PF-00547659 was developed following immunizations at Abgenix and we gratefully acknowledge the support of Sirid Kellerman and Mary Haak-Frendscho in this collaboration. We gratefully acknowledge the support of Nerviano Medical Science (Milan) in performing the cynomolgus study and Steve Martin in supporting the analysis and interpretation of the PK data.

Conflicts of interest

N Pullen, D Carter, D Finco-Kent, W Reagan, S Zhao, T Kawabata and S Sreckovic are employees of Pfizer. PF-00547659 is in Pfizer clinical development as a potential treatment for IBD.

References

Andrew DP, Berlin C, Honda S, Yoshino T, Hamann A, Holzmann B *et al.* (1994). Distinct but overlapping epitopes are involved in alpha 4 beta 7-mediated adhesion to vascular cell adhesion molecule-1, mucosal addressin-1, fibronectin, and lymphocyte aggregation. *J Immunol* **153**: 3847–3861.

Apostolaki M, Manoloukos M, Roulis M, Wurbel MA, Müller W, Papadakis KA *et al.* (2008). Role of beta7 integrin and the chemokine/chemokine receptor pair CCL25/CCR9 in modeled TNF-dependent crohns disease. *Gastroenterology* **134**: 2025–2035.

Arihiro S, Ohtani H, Suzuki M, Murata M, Ejima C, Oki M *et al.* (2002). Differential expression of mucosal addressin cell adhesion molecule-1 (MAdCAM-1) in ulcerative colitis and Crohn's disease. *Pathol Int* **52**: 367–374.

Barrett SP, Riordon A, Toh BH, Gleeson PA, van Driel IR (2000).

Homing and adhesion molecules in autoimmune gastritis. *J Leukoc Biol* **67**: 169–173.

Behm BW, Bickston SJ (2008). Tumor necrosis factor-alpha antibody for maintenance of remission in Crohn's disease. *Cochrane Database Syst Rev* CD006893. DOI: 10.1002/14651858.CD006893

Benincosa LJ, Chow FS, Tobia LP, Kwok DC, Davis CB, Jusko WJ (2000). Pharmacokinetics and pharmacodynamics of a humanized monoclonal antibody to factor IX in cynomolgus monkeys. *J Pharmacol Exp Ther* **292**: 810–816.

Berlin C, Berg EL, Briskin MJ, Andrew DP, Kilshaw PJ, Holzmann B *et al*. (1993). Alpha 4 beta 7 integrin mediates lymphocyte binding to the mucosal vascular addressin MAdCAM-1. *Cell* **74**: 185–195.

Briskin M, Winsor-Hines D, Shyjan A, Cochran N, Bloom S, Wilson J *et al*. (1997). Human mucosal addressin cell adhesion molecule-1 is preferentially expressed in intestinal tract and associated lymphoid tissue. *Am J Pathol* **151**: 97–110.

Chan BM, Elices MJ, Murphy E, Hemler ME (1992). Adhesion to vascular cell adhesion molecule 1 and fibronectin. Comparison of alpha 4 beta 1 (VLA-4) and alpha 4 beta 7 on the human B cell line JY. *J Biol Chem* **267**: 8366–8370.

Engelhardt B (2006). Molecular mechanisms involved in T cell migration across the blood- brain barrier. *J Neural Transm* **113**: 477–485.

Engelhardt B, Laschinger M, Schulz M, Samulowitz U, Vestweber D, Hoch G (1998). The development of experimental autoimmune encephalomyelitis in the mouse requires alpha4-integrin but not alpha4beta7-integrin. *J Clin Invest* **102**: 2096–2105.

Erle DJ, Briskin MJ, Butcher EC, Garcia-Pardo A, Lazarovits AI, Tidswell M (1994). Expression and function of the MAdCAM-1 receptor, integrin alpha 4 beta 7, on human leukocytes. *J Immunol* **153**: 517–528.

Farkas S, Hornung M, Sattler C, Edtinger K, Steinbauer M, Anthuber M *et al*. (2006). Blocking MAdCAM-1 in vivo reduces leukocyte extravasation and reverses chronic inflammation in experimental colitis. *Int J Colorectal Dis* **21**: 71–78.

Galfre G, Milstein C (1981). Preparation of monoclonal antibodies: strategies and procedures. *Methods Enzymol* **73** (Pt B): 3–46.

Goto A, Arimura Y, Shinomura Y, Imai K, Hinoda Y (2006). Antisense therapy of MAdCAM-1 for trinitrobenzenesulfonic acid-induced murine colitis. *Inflamm Bowel Dis* **12**: 758–765.

Green LL (1999). Antibody engineering via genetic engineering of the mouse: XenoMouse strains are a vehicle for the facile generation of therapeutic human monoclonal antibodies. *J Immunol Methods* **231**: 11–23.

Hanninen A, Jaakkola I, Jalkanen S (1998). Mucosal addressin is required for the development of diabetes in nonobese diabetic mice. *J Immunol* **160**: 6018–6025.

Hesterberg PE, Winsor-Hines D, Briskin MJ, Soler-Ferran D, Merrill C, Mackay CR *et al*. (1996). Rapid resolution of chronic colitis in the cotton-top tamarin with an antibody to a gut-homing integrin alpha 4 beta 7. *Gastroenterology* **111**: 1373–1380.

Hokari R, Kato S, Matsuzaki K, Iwai A, Kawaguchi A, Nagao S *et al*. (2001). Involvement of mucosal addressin cell adhesion molecule-1 (MAdCAM-1) in the pathogenesis of granulomatous colitis in rats. *Clin Exp Immunol* **126**: 259–265.

Kanwar JR, Kanwar RK, Wang D, Krissansen GW (2000). Prevention of a chronic progressive form of experimental autoimmune encephalomyelitis by an antibody against mucosal addressin cell adhesion molecule-1, given early in the course of disease progression. *Immunol Cell Biol* **78**: 641–645.

Kato S, Hokari R, Matsuzaki K, Iwai A, Kawaguchi A, Nagao S *et al*. (2000). Amelioration of murine experimental colitis by inhibition of mucosal addressin cell adhesion molecule-1. *J Pharmacol Exp Ther* **295**: 183–189.

Lin J, Ziring D, Desai S, Kim S, Wong M, Korin Y *et al*. (2008). TNFalpha blockade in human diseases: an overview of efficacy and safety. *Clin Immunol* **126**: 13–30.

Mager DE, Jusko WJ (2001). General pharmacokinetic model for drugs exhibiting target-mediated drug disposition. *J Pharmacokinet Pharmacodyn* **28**: 507–532.

Mullamitha SA, Ton NC, Parker GJM, Jackson A, Julyan PJ, Roberts C *et al*. (2007). Phase I evaluation of a fully human anti-{alpha}v integrin monoclonal antibody (CNTO 95) in patients with advanced solid tumors. *Clin Cancer Res* **13**: 2128–2135.

Nakache M, Berg EL, Streeter PR, Butcher EC (1989). The mucosal vascular addressin is a tissue-specific endothelial cell adhesion molecule for circulating lymphocytes. *Nature* **337**: 179–181.

Picarella D, Hurlbut P, Rottman J, Shi X, Butcher E, Ringler DJ (1997). Monoclonal antibodies specific for beta 7 integrin and mucosal addressin cell adhesion molecule-1 (MAdCAM-1) reduce inflammation in the colon of scid mice reconstituted with CD45RBhigh CD4+ T cells. *J Immunol* **158**: 2099–2106.

Pitcher CJ, Hagen SI, Walker JM, Lum R, Mitchell BL, Maino VC *et al*. (2002). Development and homeostasis of T cell memory in rhesus macaque. *J Immunol* **168**: 29–43.

Rott LS, Briskin MJ, Butcher EC (2000). Expression of alpha4beta7 and E-selectin ligand by circulating memory B cells: implications for targeted trafficking to mucosal and systemic sites. *J Leukoc Biol* : 807–814.

Sandborn WJ, Colombel JF, Enns R, Feagan BG, Hanauer SB, Lawrance IC *et al*. (2005). Natalizumab induction and maintenance therapy for Crohn's disease. *N Engl J Med* **353**: 1912–1925.

Shigematsu T, Specian RD, Wolf RE, Grisham MB, Granger DN (2001). MAdCAM mediates lymphocyte-endothelial cell adhesion in a murine model of chronic colitis. *Am J Physiol Gastrointest Liver Physiol* **281**: G1309–G1315.

Shyjan AM, Bertagnolli M, Kenney CJ, Briskin MJ (1996). Human mucosal addressin cell adhesion molecule-1 (MAdCAM-1) demonstrates structural and functional similarities to the alpha 4 beta 7-integrin binding domains of murine MAdCAM-1, but extreme divergence of mucin-like sequences. *J Immunol* **156**: 2851–2857.

Simmons DL (1993). Cloning cell surface molecules by transient expression in mammalian cells. In: Hartley DA (ed.). *Cellular Interactions in Development: A Practical Approach*. Oxford University Press: Oxford, pp. 93–127.

Souza HS, Elia CC, Spencer J, MacDonald TT (1999). Expression of lymphocyte-endothelial receptor-ligand pairs, alpha4beta7/MAdCAM-1 and OX40/OX40 ligand in the colon and jejunum of patients with inflammatory bowel disease. *Gut* **45**: 856–863.

Steffen BJ, Breier G, Butcher EC, Schulz M, Engelhardt B (1996). ICAM-1, VCAM-1, and MAdCAM-1 are expressed on choroid plexus epithelium but not endothelium and mediate binding of lymphocytes in vitro. *Am J Pathol* **148**: 1819–1838.

Streeter PR, Berg EL, Rouse BT, Bargatze RF, Butcher EC (1988). A tissue-specific endothelial cell molecule involved in lymphocyte homing. *Nature* **331**: 41–46.

Targan SR, Feagan BG, Fedorak RN, Lashner BA, Panaccione R, Present DH *et al*. (2007). Natalizumab for the treatment of active Crohn's disease: results of the ENCORE Trial. *Gastroenterology* **132**: 1672–1683.

Van Assche G, Van Ranst M, Sciot R, Dubois B, Vermeire S, Noman M *et al*. (2005). Progressive multifocal leukoencephalopathy after natalizumab therapy for Crohn's disease. *N Engl J Med* **353**: 362–368.

Wu B, Joshi A, Ren S, Ng C (2006). The application of mechanism-based PK/PD modeling in pharmacodynamic-based dose selection of muM17, a surrogate monoclonal antibody for efalizumab. *J Pharm Sci* **95**: 1258–1268.

Yang XD, Sytwu HK, McDevitt HO, Michie SA (1997). Involvement of beta 7 integrin and mucosal addressin cell adhesion molecule-1 (MAdCAM-1) in the development of diabetes in obese diabetic mice. *Diabetes* **46**: 1542–1547.